Brain Imaging and Behavior (2019) 13:1602–1611
https://doi.org/10.1007/s11682-019-00144-1

ORIGINAL RESEARCH

Behavioral inhibition corresponds to white matter fiber bundle integrity in older adults

Paola M. Garcia-Egan[1] · Rebecca N. Preston-Campbell[2] · Lauren E. Salminen[3] · Jodi M. Heaps-Woodruff[2] · Lila Balla[2] · Ryan P. Cabeen[4] · David H. Laidlaw[5] · Thomas E. Conturo[6] · Robert H. Paul[1,2]

Published online: 17 June 2019

Abstract

Little is known about the contribution of white matter integrity to inhibitory cognitive control, particularly in healthy aging. The present study examines the correspondence between white matter fiber bundle length and behavioral inhibition in 37 community-dwelling older adults (aged 51–78 years). Participants underwent neuroimaging with 3 Tesla MRI, and completed a behavioral test of inhibition (i.e., Go/NoGo task). Quantitative tractography derived from diffusion tensor imaging (qtDTI) was used to measure white matter fiber bundle lengths (FBLs) in tracts known to innervate frontal brain regions, including the anterior corpus callosum (AntCC), the cingulate gyrus segment of the cingulum bundle (CING), uncinate fasciculus (UNC), and the superior longitudinal fasciculus (SLF). Performance on the Go/NoGo task was measured by the number of commission errors standardized to reaction time. Hierarchical regression models revealed that shorter FBLs in the CING ($p < 0.05$) and the bilateral UNC ($p < 0.01$) were associated with lower inhibitory performance after adjusting for multiple comparisons, supporting a disconnection model of response inhibition in older adults. Prospective longitudinal studies are needed to examine the evolution of inhibitory errors in older adult populations and potential for therapeutic intervention.

Keywords Inhibition · Go/NoGo · White matter · Quantitative diffusion tensor imaging · MRI fiber bundle length · Aging

Introduction

White matter (WM) integrity has been shown to be associated with reduced cognitive function in older adults (Madden et al. 2009; Madden et al. 2012). In particular, executive functions that require fast reaction time, such as behavioral inhibition, are vulnerable to age-related compromise (Jacobs et al. 2013; Lee et al. 2012; Lu et al. 2013). Behavioral inhibition refers to the ability to withhold an automatic response, or to resist enticing behaviors (Casey et al. 1997; Menon et al. 2001; Hirose et al. 2012; Dambacher et al. 2014). This higher-order skill in executive function depends on efficient transmission of information across the brain, with predominate involvement of frontal-cortical regions, including the fronto-parietal, fronto–temporal, and frontal-subcortical networks (Rubia et al. 2001; Zhang and Li 2012; Hong et al. 2016; Steele et al. 2013; van Gaal et al. 2010; Angelini et al. 2015; Garavan et al. 1999).

Studies using MRI diffusion tensor imaging (DTI) reveal that the microstructural integrity of the superior longitudinal fasciculus, uncinate fasciculus (UNC), cingulate gyrus segment of the cingulum, and tracts connecting the inferior frontal gyrus with the subcortical structures, are key anatomical substrates of inhibitory control (Rizk et al. 2017; Sasson et al. 2013; Hinton et al. 2018). Compared to functional neuroimaging measures, indices of structural connectivity (e.g., white matter fractional anisotropy; FA) account for age-related variance in inhibitory performance (Fjell, Sneve, Gryndeland, Storsve and Walhovd 2016).

✉ Robert H. Paul
paulro@umsl.edu

1 Department of Psychological Sciences, University of Missouri, St. Louis, MO 63121, USA

2 Missouri Institute of Mental Health, St. Louis, MO 63134, USA

3 Imaging Genetics Center, Stevens Neuroimaging and Informatics Institute, University of Southern California, Marina del Rey, CA 90292, USA

4 Laboratory of Neuro Imaging, Stevens Neuroimaging and Informatics Institute, Keck School of Medicine of USC, University of Southern California, LosAngeles, CA 90033, USA

5 Department of Computer Science, Brown University, Providence, RI 02906, USA

6 Mallinckrodt Institute of Radiology, Washington University School of Medicine, St. Louis, MO 63110, USA

In previous studies, we described the sensitivity of quantitative diffusion tensor imaging (qDTI) in which we used DTI-based tractography to measure fiber bundle lengths (FBLs) in older individuals (Baker et al. 2014). In this approach, each streamline obtained by tractography is taken to represent a statistical summary of a local bundle of parallel-packed neuronal fibers, from which, the overall arc-length of the trajectory of each fiber bundle is measured (Correia et al. 2008). Additionally, the microstructural properties of the fiber bundles are assessed by measuring the DTI metrics along the entire length of each fiber bundle. This approach combines tractography and DTI scalar metrics to characterize the structural properties of fiber bundles that make up a WM tract. DTI metrics such as FA and mean diffusivity (MD) are usually averaged at the voxel or regional level and single tensor models only measure the directionality of tracts along a primary eigenvector, which lacks information relevant to the organization and microstructure of white matter tracts. In contrast, FBLs are derived from scalar DTI metrics, such as FA, in combination with tractography methods to trace white matter fibers (Correia et al. 2008). Such an approach can detect properties that may be undetected by traditional regional measures of scalar DTI metrics (Correia et al. 2008; Hasan et al. 2009), and reveal additional alterations in white matter integrity that correspond to cognitive decline (Behrman-Lay et al. 2014; Salminen et al. 2016.

Using this approach, older individuals without clinically evident neurodegeneration exhibit reduced FBLs compared to younger adults (Baker et al. 2014; Bolzenius et al. 2013). Moreover, the age-associated shortening of FBL corresponds to worse performance in domains of cognition that are vulnerable to age (Behrman-Lay et al. 2014; Salminen et al. 2013; Salminen et al. 2016; Baker et al. 2017). In particular, we found a relation between shorter FBLs and reduced processing speed (Behrman-Lay et al. 2014; Salminen et al. 2016). To date, no study has utilized the innovative imaging metric of FBL to examine the white matter signature of inhibitory cognitive performance in older adults.

Postmortem studies report reduced length of frontal axonal bundles are reduced in older individuals (Marner et al. 2003; Tang et al. 1997), suggesting that alterations in the structural connectome of the brain may underlie an age-related a decline in cognitive performance (Behrman-Lay et al. 2014). The present study examined FBLs in four tracts of interest (TOIs) that project to the frontal cortex and have been independently associated with inhibitory control. For example, prior studies using common DTI scalar metrics reveal associations between worse inhibitory performance and lower FA in the anterior corpus callosum (AntCC) and the uncinate fasciculus (UF) (Salo et al. 2009; Hornberger et al. 2011). Higher diffusivity in the cingulate gyrus segment of the cingulum bundle (CING) and the superior longitudinal fasciculus (SLF) also correspond to worse performance on the Go/NoGo task (Colrain et al. 2011; Sasso et al. 2013). Based on our above prior studies of FBL, aging, and cognition, we hypothesized that longer FBLs would correspond with better inhibitory performance.

Methods

Participants

A total of 37 healthy older adults between the ages of 51–78 years were included in the study (males $n = 9$, females $n = 28$). Participants were all English-speaking individuals and predominantly White/Caucasian ($n = 26$, Black/African American $n = 8$, and other $n = 3$), with an average education level of 16 years. Exclusion criteria included: 1) a score of <24 on the Mini-Mental State Examination (MMSE; Folstein et al. 1975), 2) evidence of neurologic disease, 3) past head injury with loss of consciousness >5 min, 4) severe medical illnesses (e.g., cancer, treatment-dependent diabetes), 4) any Axis I and/or Axis II psychiatric disorders with the exception of treated depression, 5) past or present substance use disorder, 6) any hearing, vision, or motor impairment that precluded cognitive testing, and 7) contraindications for MRI. All participants completed neuropsychological testing within one month of the neuroimaging protocol. The average time between the neuroimaging and neuropsychological evaluations was 23 days. The recruiting methods and total population from which the sample was derived are described in (Paul et al. 2011). Written informed consent was obtained prior to study participation. Participants received financial compensation for their involvement. The Institutional Review Board at the corresponding universities approved the study.

Go/NoGo task

A computerized Go/NoGo task was administered in a sound-controlled room. The task required participants to respond repeatedly to target stimuli (Go), and inhibit the prepotent response when non-target stimuli (NoGo) appeared (Beck et al. 1956). The word "PRESS" was displayed on the screen for 500 ms, with a one second inter-stimulus interval. Participants were instructed to press a button with their index finger as quickly as possible when "PRESS" was presented in green font (Go), and to not respond when the word was presented in red font (NoGo). Speed and accuracy of response was equally stressed in the task instructions (Gordon et al. 2005; Paul et al. 2005). Six trials of 28 stimulus presentations were presented in pseudo-random order, for a total of 168 trials. The ratio of Go to NoGo trials was 75:25. Prior to the task, participants completed a brief practice session. Reaction time was recorded continuously for the duration of the task (6 min), but not on a trial-by-trial basis.

To minimize conflation between commission errors and response speed (Bruyer and Brysbaert 2011; Jones et al.

2016; Bezdjian et al. 2009; Menon et al. 2001; Steele et al. 2013), a composite score of task accuracy and response latency was calculated using the rate residual scoring method (Hirose et al. 2012; Hughes, Linck, Bowles, Koeth and Bunting 2014; Was and Woltz 2007; Woltz and Was 2006). Briefly, a regression line was fit between the average reaction time and the number of false positive errors for all subjects, dividing participants with faster reaction times and fewer errors (below the line = negative scores) from participants with a longer reaction time and/or more errors (above the line = positive scores). The regression line between reaction time and the NoGo errors was used to calculate the inhibitory performance score. The distribution of performances (depicted by dots) represents the distance to the line (Fig. 1).

MRI data acquisition

All participants were scanned at a single site using a head-only Magnetom Allegra 3 T MRI (Siemens Medical Solutions, Erlangen, Germany) with a standard imaging protocol that included a diffusion-weighted MRI sequence. Head positioning was confirmed by a preliminary scout scan composed of three orthogonal planes collected from each individual at the beginning of the scanning procedure. Movement artefact was limited by application of surgical tape across the forehead to enhance stability. High-performance gradients (maximum strength 40 mT/m in a 100-ms rise time; maximum slew rate 400 T/m/s) were utilized to minimize scan times (< 1 h). FSL BET was used to extract whole brain masks for each subject, and intracranial volume (ICV) was computed from the total volume inside the mask (Jenkinson et al. 2012).

Diffusion-weighted imaging acquisition

A customized in-house single-shot multislice echo-planar pulse sequence was utilized to acquire the axial diffusion-weighted images. The tensor was encoded using 31 non-collinear directions were utilized, with 24 main directions aligned with the applied diffusion gradient ($b = 996$ s/mm^2). A "core" of tetrahedral directions (Conturo et al. 1996) was used to maximize the signal-to-noise rate (SNR) efficiency and directional coverage, with 5 baseline I_0 acquisitions ($b \approx 0$). The following parameters were used: TE = 86.2 ms; TR = 7.82 s; 64 contiguous 2.0-mm slices; and an acquisition matrix of 128 X 128 with a field of view of 256 X 256 mm (isotropic 2.0 X 2.0 X 2.0 mm voxels). Signal was averaged from 72 acquisitions. Further scan acquisition details are described in our prior studies (Baker et al. 2016; Behrman-Lay et al. 2014; Bolzenius et al. 2013; Salminen et al. 2016).

Quantitative diffusion tractography (qtDTI)

Diffusion-weighted volumes were preprocessed using FSL 5.0 (Jenkinson et al. 2012) and the Quantitative Imaging Toolkit (QIT) (Cabeen et al. 2018). The images were corrected for motion and eddy-current induced artifacts through affine

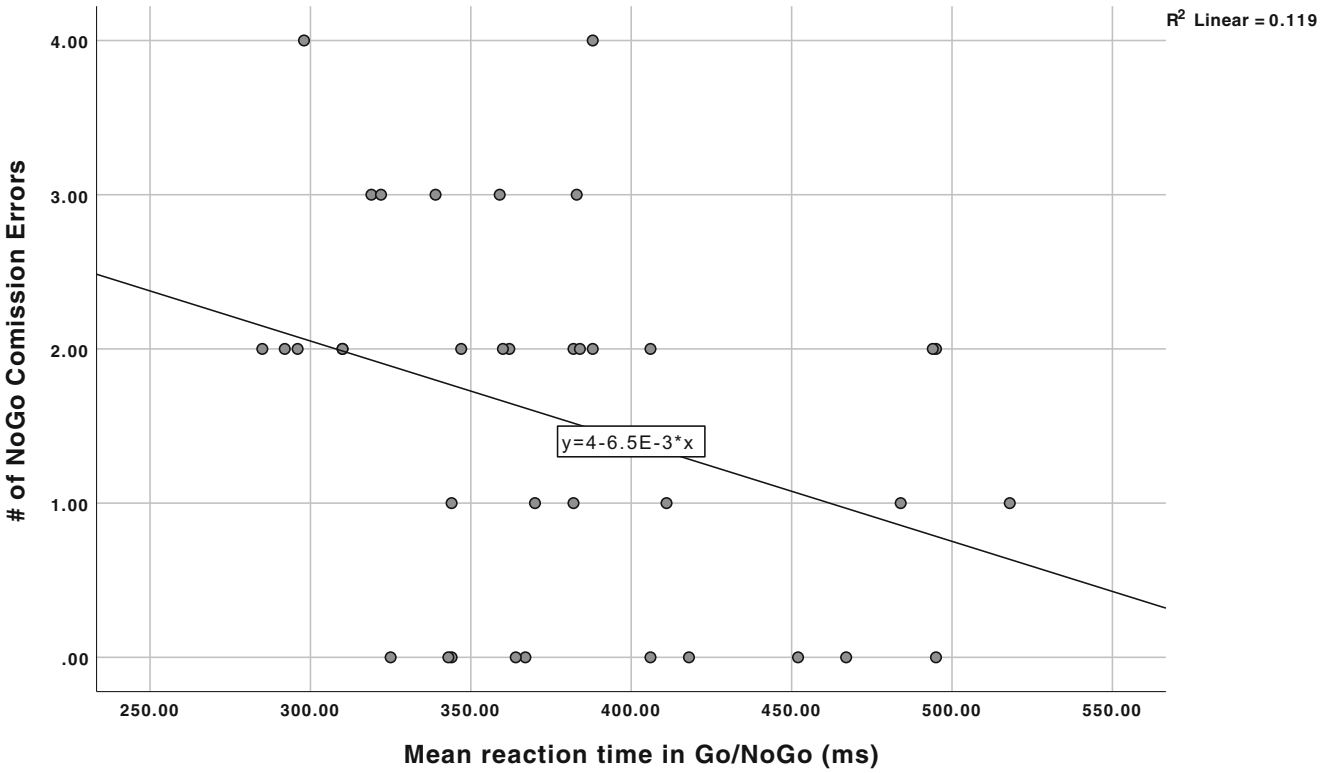

Fig. 1 Regression of overall reaction time and commission errors

registration to the first baseline volume using FSL FLIRT (Jenkinson and Smith 2001) with the mutual information criteria. The orientations of the gradient encoding directions were corrected by the rotation induced by these registrations (Leemans and Jones 2009), and brain tissue was extracted using FSL BET (Smith 2002) with a fraction threshold of 0.45. Diffusion tensor images were estimated for each subject using FSL DTIFIT and a study-specific white matter atlas was created using DTI-TK (Zhang et al. 2007). The template image was computed by iteratively deforming and averaging the sample imaging data using the tensor-based deformable registration algorithm in DTI-TK (Zhang et al. 2006) with finite strain tensor reorientation and the deviatoric tensor similarity metric. This template was used to define the AntCC, bilateral CING, bilateral UF, and bilateral SLF (Mori and van Zijl 2002).

Specificity of fiber extraction is difficult without tractography maps, due the heterogeneity and convoluted nature of WM bundles. Therefore, we used a template-based approach to extract subject-specific fiber bundle models; specifically, whole brain tractography was performed in the subject native space, and subsets of curves were selected using template masks to select each bundle-of-interest (Zhang et al. 2010). For each bundle-of-interest, two inclusion region of interests (ROIs) and one exclusion ROI were drawn in template space using ITK-SNAP (Yushkevich et al. 2006). These masks were placed at opposite ends of each bundle, and then drawn in reference to standard white matter atlases (Catani and de Schotten 2012). Tractography was performed in subject native space using deterministic streamline integration using QIT (Zhang et al. 2003) with a step size of 1 mm, tricubic interpolation, and four jittered seeds per voxel. Termination criteria included an angle threshold of 45 degrees and minimum FA of 0.15. Fiber curves with lengths less than 10 mm were excluded from the analysis. FBLs were computed from the resulting curves (Correia et al. 2008). Corrections for head size were made by dividing FLB measures by the ratio of participants' ICV to the sample average ICV (Correia et al. 2008). Representation of TOIs is shown in Fig. 2.

Statistical analyses

Statistical analyses were conducted in SPSS 25 (IBM Corp 2017). The Shapiro-Wilk Tests of normality were performed, and skewness and kurtosis scores were evaluated to assess for normal distribution of the data. Group differences in age and education between "good" and "poor" performers were examined using independent-samples t-tests; Chi-square tests examined differences in sex and ethnicity. Preliminary analyses revealed skewed distributions for age, reaction time, omission errors, inhibitory errors, AntCC, SLF and CING, therefore, the p value was calculated based on 1000 bootstraps to correct for potential deviation from the Gaussian distribution (Pavlov et al. 2010; Haukoos and Lewis 2005). The Shapiro-Wilk test ($p = 0.53$) revealed that the distribution of inhibitory performance scores was similar to a Gaussian distribution; the SD of the distribution of the inhibitory performance score was 0.97 (Fig. 3). The purpose of correlations analysis was to establish whether age and education should be included in the regression model, correlations were conducted to examine associations with TOIs.

Inspection of diagnostic plots (Q–Q plots and residual plots) and diagnostic statistical values (Cook's distance

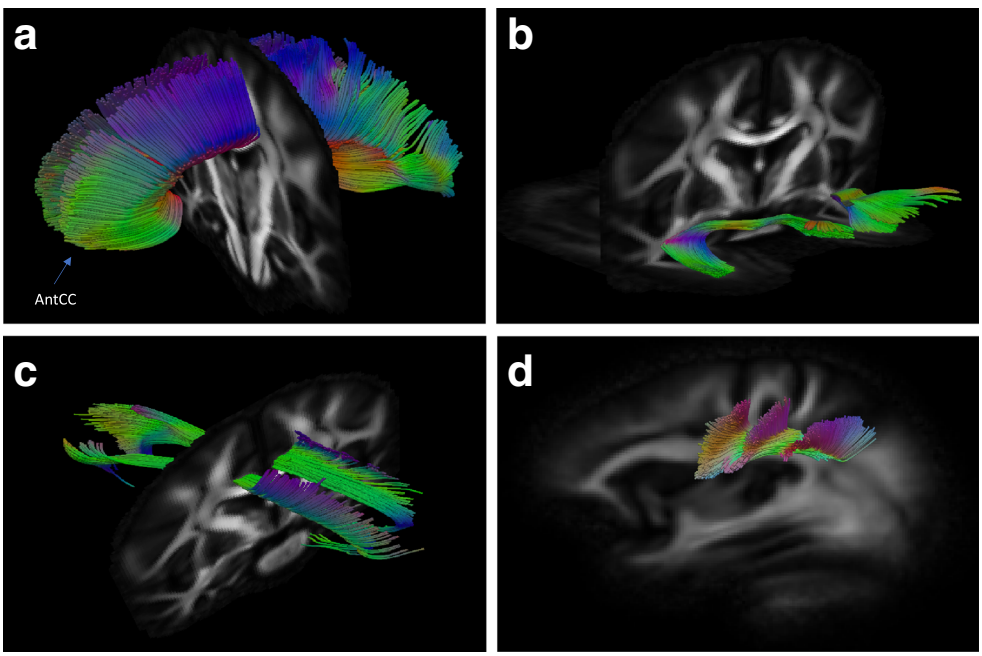

Fig. 2 Reconstruction of white matter tracts of interest using qtDTI in coronal plane view: **a**) Anterior corpus callosum (AntCC). **b**) Uncinate fasciculus. **c**) Cingulum bundle. In sagittal plane view: **d**) Superior longitudinal fasciculus

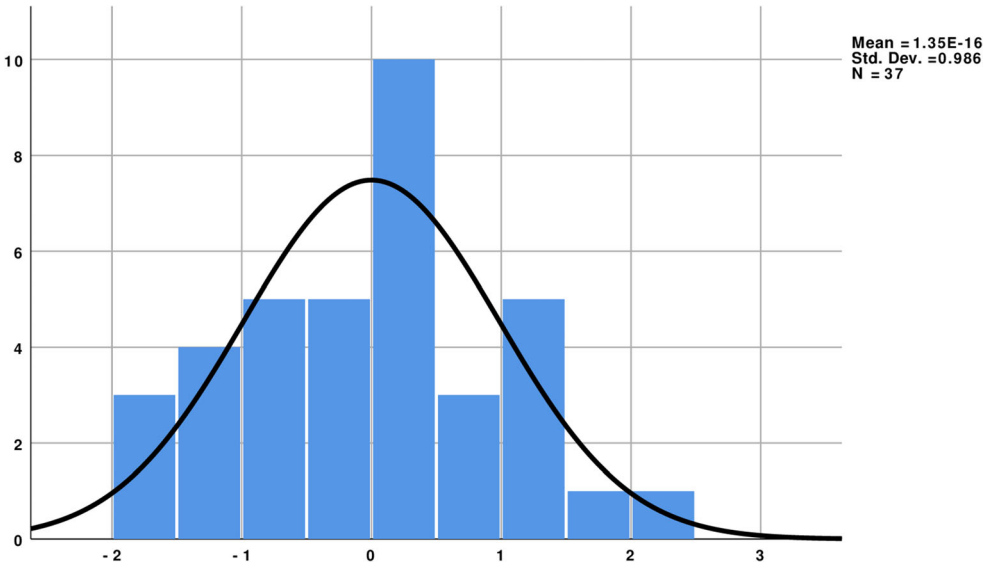

Fig. 3 Distribution of regression standardized values as efficiency index scores

<1, variance inflation factor < 4) revealed no violations of the statistical assumptions. As such, hierarchical regression analysis was used to determine the association between the composite score of inhibitory performance on the Go/NoGo task with each TOI. To address whether specific TOIs were associated significantly with Go/NoGo performance after adjusting for age, we conducted structured hierarchical regression models for each TOI, with age in the first block, and inhibitory performance entered in the second block. The data are presented as mean ± standard deviation (SD) or median and interquartile range (IQR) for non-normal distributed variables. Bootstrapped significance was set as $p < 0.05$. The False Discovery Rate (FDR) procedure was used to correct for multiple comparisons (Benjamini and Hochberg 1995).

Results

Demographic characteristics of the sample are reported in Table 1. Results of the correlations showed a relationship between inhibitory performance and FBL in the CING and the UNC (Table 2). However, no association between age and TOIs, and education and TOIs emerged. Results of the hierarchical structured regression revealed that inhibitory performance was significantly associated with FBLs in the CING (Adjusted $R^2 = 0.124$; $p = 0.021$) and the UNC (Adjusted $R^2 = 0.247$; $p = 0.006$) after FDR corrections, but not with the AntCC (Adjusted $R^2 = 0.103$; $p = 0.114$) and SLF (Adjusted $R^2 = 0.145$; $p = 0.083$) (Table 3).

Fiber bundle lengths corrected for head size, SD: standard deviation, IQR: interquartile range, MMSE: Mini–Mental State Examination.

Table 1 Demographic information, cognition and mean fiber bundle length (mm) in the sample ($N = 37$)

Variable	Mean/ Median	SD/ IQR	Minimum	Maximum
Demographics				
Age	59.00	12.50	51	78
Education	15.81	2.38	12	20
Cognition				
MMSE	28.84	1.67	26	30
Go/NoGo Reaction Time (ms)	367.00	76.50	285	518
Commission (NoGo) Errors	2.00	2	0	4
Omission (Go) Errors	1	2.5	0	24
Fiber bundle lengths				
Anterior corpus callosum	99.79	15.33	70.87	154.34
Cingulum	86.05	17.31	61.21	125.70
Uncinate Fasciculus	66.55	12.89	39.14	95.69
Superior longitudinal fasciculus	68.37	11.13	53.21	98.97

Table 2 Correlations of mean fiber bundle length, demographics, and efficiency score index

Variables	AntCC *r*	CING *r*	UF *r*	SLF *r*
Age	−0.167	−0.091	0.057	−0.131
Education	−0.013	−0.073	−0.244	−0.026
Inhibitory performance score	−0.286	−0.411*	−0.497**	−0.366

*$p < 0.05$, ** $p = < 0.01$

Discussion

This is the first study using qtDTI to investigate the white matter substrate of inhibition in healthy older adults. Our results show that shorter FBL of the UNC tract and the CING correlate with lower inhibitory performance, when accounting for speed-accuracy trade-offs. These results provide empirical support for a disconnection model of inhibition in a healthy aging population (Greenwood 2000; O'Sullivan et al. 2001; Charlton et al. 2006; Madden et al. 2017; Fjell et al. 2017; Salat et al. 2005).

The association between inhibition and the UNC in the present study is noteworthy. The UNC connects the frontal lobe (primarily the orbitofrontal cortex) to the anterior temporal lobe, including the amygdala and hippocampus (Kier et al. 2004). In healthy adults, lower performance on the Go/NoGo and Stroop tests are significantly associated with decreased WM microstructural integrity of the UNC (Sasson et al. 2013). These results provide empirical support for a disconnection model of inhibition in a healthy aging population (Greenwood 2000; O'Sullivan et al. 2001; Charlton et al. 2006; Madden et al. 2017; Fjell et al. 2017; Salat et al. 2005). The disconnection theory of aging proposes that age-related cognitive decline results predominately from degenerated connections between cortical regions rather than focal degeneration within a cortical region. Between the ages of 20 through 80, myelinated fibers are shortened by 50% (Marner et al. 2003). It is estimated that these fibers shorten at a rate of 10% per decade (Tang et al. 1997). Shortened axon bundles are believed to underlie mechanisms of age-related cognitive decline (Catani 2006).

The observation that FBL in the CING corresponds to inhibition is consistent with prior studies in healthy participants (Rizk et al. 2017; Metzler-Baddeley et al. 2012), as well as clinical populations (Murphy et al. 2007, Kubicki et al. 2009, Hornberger et al. 2011). Anatomically, the CING is connected to frontal, parietal, and medial temporal sites, as well as subcortical nuclei (Schmahmann and Pandya 2006), all of which are essential for executive control (self-monitoring and evaluation of performance) and processing speed (Yang et al. 2016; Sasson et al. 2013).

Axonal degeneration among generally healthy older adults is likely associated with demyelination secondary to

Table 3 Hierarchical multiple regression models of qtDTI metrics of 4 TOIs and efficiency index scores when controlling for age

Predictor	Anterior corpus callosum				Cingulum				Uncinate fasciculus				Superior longitudinal fasciculus			
	R^2 change	F change	β	SE	R^2 change	F change	β	SE	R^2 change	F change	β	SE	R^2 change	F change	β	SE
Step 1	0.03	1.00			0.01	0.29			0.00	0.11			0.02	0.61		
Age			−0.38	0.33			−.176	0.281			−0.09	0.25			−0.20	0.24
Step 2	0.07	2.86			0.16*	6.76			0.24**	11.03			0.128	5.09		
Age			−0.33	0.33			−0.120	0.217			−0.03	0.23			−0.16	0.23
Inhibitory performance score			−4.22	3.11			−6.13*	2.51			−6.48**	2.04			−4.28	2.34

*$p < 0.05$, ** $p = < 0.01$. Results are significant after FDR corrections

inflammation and oxidative stress (Pan and Chan 2017). As reflected in studies with healthy older adults, decreased FA and increased MD are common findings in studies of older brains (Inano et al. 2011; Bennett et al. 2011; Westlye et al. 2009; Sexton et al. 2014; Bender et al. 2016; Charlton et al. 2010). These age effects are probably driven by changes in underlying myelin, as suggested by consistently shown age-related increases in radial diffusivity, whereas axial diffusivity changes less consistently observed (Sullivan et al. 2010; Zahr et al. 2009; Davis et al. 2009; Phillips et al. 2013; Inano et al. 2011). More studies using advanced microstructural modeling techniques, such as Neurite Orientation Dispersion and Density Imaging (Zhang et al. 2012) are needed to address this question.

Although there is increasing interest in qtDTI, we acknowledge there are some limitations related to this technique. We used affine registration, which may have resulted in missed fibers or the inclusion of extra fibers that terminate at regions distant from the WM-gray matter boundary. Complex WM configurations are not well characterized by single-tensor modeling, and multi-compartment diffusion may offer more anatomically accurate results (Cabeen et al. 2016). Similarly, the anatomical precision of FBLs could be enhanced by high angular resolution diffusion. The age of the sample was fairly young and the range was limited, which may have accounted for the absence of a clear age effect. Furthermore, our sample was relatively small and may not be representative of the population. Longitudinal studies utilizing multiple measures of inhibitory control in a larger sample of older individuals are needed to the generalizability of the results in other elderly cohorts.

Conclusion

The present study revealed that WM integrity of the UNC and left CING correspond to behavioral inhibition among healthy older adults. The results support a disconnection model of cognitive aging. Additional studies using a prospective design are needed to define the development of inhibitory performance errors in older adults and determine the real-world relevance of such errors in everyday living skills.

Funding Supported by National Institutes of Health/National Institute of Neurological Disorders and Stroke grant number R01 NS052470 and R01 NS039538, National Institutes of Health/National Institute of Mental Health grant R21 MH090494.

Compliance with ethical standards

Conflict of interest Drs. Paul, Heaps, Salminen, Preston-Campbell, Cabeen, Laidlaw, Conturo, and Ms. García-Egan declare no conflicts of interest.

Informed consent All procedures were in accordance with the ethical standards of the responsible committee in research involving human subjects (Institutional and national) and with the Helsinki Declaration of 1975, and the applicable revisions at the time of the investigation. Informed consent was obtained from all participants.

References

Angelini, M., Calbi, M., Ferrari, A., Sbriscia-Fioretti, B., Franca, M., Gallese, V., & Umiltà, M. A. (2015). Motor inhibition during overt and covert actions: An electrical neuroimaging study. *PLoS One, 10*(5). https://doi.org/10.1371/journal.pone.0126800.

Baker, L. M., Laidlaw, D. H., Conturo, T. E., Hogan, J., Zhao, Y., Luo, X., Correia, S., Cabeen, R., Lane, E. M., Heaps, J. M., Bolzenius, J., Salminen, L. E., Akbudak, E., McMichael, A. R., Usher, C., Behrman, A., & Paul, R. H. (2014). White matter changes with age utilizing quantitative diffusion MRI. *Neurology, 83*(3), 247–252.

Baker, L. M., Cabeen, R. P., Cooley, S. A., Laidlaw, D. H., & Paul, R. H. (2016). Application of a novel quantitative tractography-based analysis of diffusion tensor imaging to examine fiber bundle length in human cerebral white matter. *Technology and Innovation, 18*, 21–29.

Baker, L. M., Laidlaw, D. H., Cabeen, R., Akbudak, E., Conturo, T. E., Correia, S., et al. (2017). Cognitive reserve moderates the relationship between neuropsychological performance and white matter fiber bundle length in healthy older adults. *Brain Imaging and Behavior, 11*(3), 632–639.

Beck, L. H., Bransome, E. D., Jr., Mirsky, A. F., Rosvold, H. E., & Sarason, I. (1956). A continuous performance test of brain damage. *Journal of Consulting Psychology, 20*(5), 343–350.

Behrman-Lay, A. M., Usher, C., Conturo, T. E., Correia, S., Laidlaw, D. H., Lane, E. M., et al. (2014). Fiber bundle length and cognition: A length-based tractography MRI study. *Brain Imaging and Behavior., 9*(4), 765–775.

Bender, A. R., Völkle, M. C., & Raz, N. (2016). Differential aging of cerebral white matter in middle-aged and older adults: A seven-year follow-up. *Neuroimage, 125*, 74–83.

Benjamini, Y., & Hochberg, Y. (1995). Controlling the false discovery rate: A practical and powerful approach to multiple testing. *Journal of the Royal Statistical Society. Series B (Methodological), 57*, 289–300.

Bennett, I. J., Madden, D. J., Vaidya, C. J., Howard, J. H., Jr., & Howard, D. V. (2011). White matter integrity correlates of implicit sequence learning in healthy aging. *Neurobiology of Aging, 32*(12), 2317–23e1.

Bezdjian, S., Baker, L. A., Lozano, D. I., & Raine, A. (2009). Assessing inattention and impulsivity in children during the go/NoGo task. *British Journal of Developmental Psychology, 27*(2), 365–383.

Bolzenius, J. D., Laidlaw, D. H., Cabeen, R. P., Conturo, T. E., McMichael, A. R., Lane, E. M., Heaps, J. M., Salminen, L. E., Baker, L. M., Gunstad, J., & Paul, R. H. (2013). Impact of body mass index on neuronal fiber bundle lengths among healthy older adults. *Brain Imaging Behavior, 7*(3), 300–306.

Bruyer, R., & Brysbaert, M. (2011). Combining speed and accuracy in cognitive psychology: Is the inverse efficiency score (IES) a better dependent variable than the mean reaction time (RT) and the percentage of errors (PE)? *Psychologica Belgica, 51*(1), 5–13.

Cabeen, R. P., Bastin, M. E., & Laidlaw, D. H. (2016). Kernel regression estimation of fiber orientation mixtures in diffusion MRI. *Neuroimage, 127*, 158–172.

Cabeen, R. P., Laidlaw, D. H., & Toga, A. W. (2018). Quantitative imaging toolkit: Software for interactive 3D visualization, data exploration, and computational analysis of neuroimaging datasets. In

Proceedings of the joint annual meeting ISMRM-ESMRMB (p. 2854). Paris, France.

Casey, B. J., Trainor, R. J., Orendi, J. L., Schubert, A. B., Nystrom, L. E., Giedd, J. N., Castellanos, F. X., Haxby, J. V., Noll, D. C., Cohen, J. D., Forman, S. D., Dahl, R. E., & Rapoport, J. L. (1997). A developmental functional MRI study of prefrontal activation during performance of a go-no-go task. *Journal of Cognitive Neuroscience, 9*(6), 835–847.

Catani, M. (2006). Diffusion tensor magnetic resonance imaging tractography in cognitive disorders. *Current Opinion in Neurology, 19*(6), 599–606.

Catani, M., & de Schotten, M. T. (2012). *Atlas of human brain connections*. Oxford University Press.

Charlton, R. A., Barrick, T. R., McIntyre, D. J., Shen, Y., O'sullivan, M., Howe, F. E. E. A., et al. (2006). White matter damage on diffusion tensor imaging correlates with age-related cognitive decline. *Neurology, 66*(2), 217–222.

Charlton, R. A., Schiavone, F., Barrick, T. R., Morris, R. G., & Markus, H. S. (2010). Diffusion tensor imaging detects age related white matter change over a 2 year follow-up which is associated with working memory decline. *Journal of Neurology, Neurosurgery & Psychiatry, 81*(1), 13–19.

Colrain, I. M., Sullivan, E. V., Ford, J. M., Mathalon, D. H., McPherson, S.-L., Roach, B. J., Crowley, K. E., & Pfefferbaum, A. (2011). Frontally mediated inhibitory processing and white matter microstructure: Age and alcoholism effects. *Psychopharmacology, 213*(4), 669–679.

Conturo, T. E., McKinstry, R. C., Akbudak, E., & Robinson, B. H. (1996). Encoding of anisotropic diffusion with tetrahedral gradients: A general mathematical diffusion formalism and experimental results. *Magnetic Resonance in Medicine, 35*(3), 399–412.

Corp, I. B. M. (2017). *IBM SPSS statistics for windows, version 25.0*. Armonk, NY: IBM Corp.

Correia, S., Lee, S. Y., Voorn, T., Tate, D. F., Paul, R. H., Zhang, S., Salloway, S. P., Malloy, P. F., & Laidlaw, D. H. (2008). Quantitative tractography metrics of white matter integrity in diffusion-tensor MRI. *Neuroimage, 42*(2), 568–581.

Dambacher, F., Sack, A. T., Lobbestael, J., Arntz, A., Brugmann, S., & Schuhmann, T. (2014). The role of right prefrontal and medial cortex in response inhibition: Interfering with action restraint and action cancellation using transcranial magnetic brain stimulation. *Journal of Cognitive Neuroscience, 26*(8), 1775–1784. https://doi.org/10.1162/jocn_a_00595.

Davis, S. W., Dennis, N. A., Buchler, N. G., White, L. E., Madden, D. J., & Cabeza, R. (2009). Assessing the effects of age on long white matter tracts using diffusion tensor tractography. *Neuroimage, 46*(2), 530–541.

Fjell, A. M., Sneve, M. H., Grydeland, H., Storsve, A. B., & Walhovd, K. B. (2016). The disconnected brain and executive function decline in aging. *Cerebral Cortex, 27*(3), 2303–2317.

Folstein, M. F., Folstein, S. E., & McHugh, P. R. (1975). "Mini-mental state": A practical method for grading the cognitive state of patients for the clinician. *Journal of Psychiatric Research, 12*(3), 189–198.

Garavan, H., Ross, T. J., & Stein, E. A. (1999). Right hemispheric dominance of inhibitory control: An event-related functional MRI study. *Proceedings of the National Academy of Science of the USA, 96*(14), 8301–8306.

Gordon, E., Cooper, N., Rennie, C., Hermens, D., & Williams, L. M. (2005). Integrative neuroscience: The role of a standardized database. *Clinical EEG and Neuroscience, 36*(2), 64–75.

Greenwood, P. M. (2000). The frontal aging hypothesis evaluated. *Journal of the International Neuropsychological Society, 6*(6), 705–726.

Hasan, K. M., Iftikhar, A., Kamali, A., Kramer, L. A., Ashtari, M., Cirino, P. T., Papanicolaou, A. C., Fletcher, J. M., & Ewing-Cobbs, L. (2009). Development and aging of the healthy human brain uncinate fasciculus across the lifespan using diffusion tensor tractography. *Brain Research, 1276*, 67–76.

Haukoos, J. S., & Lewis, R. J. (2005). Advanced statistics: Bootstrapping confidence intervals for statistics with "difficult" distributions. *Academic Emergency Medicine, 12*(4), 360–365.

Hinton, K. E., Lahey, B. B., Villalta-Gil, V., Boyd, B. D., Yvernault, B. C., Werts, K. B., Plassard, A. J., Applegate, B., Woodward, N. D., Landman, B. A., & Zald, D. H. (2018). Right fronto-subcortical white matter microstructure predicts cognitive control ability on the go/no-go task in a community sample. *Frontiers in Human Neuroscience, 12*, 127.

Hirose, S., Chikazoe, J., Watanabe, T., Jimura, K., Kunimatsu, A., Abe, O., Ohtomo, K., Miyashita, Y., & Konishi, S. (2012). Efficiency of go/no-go task performance implemented in the left hemisphere. *Journal of Neuroscience, 32*(26), 9059–9065.

Hong, X., Liu, Y., Sun, J., & Tong, S. (2016). Age-related differences in the modulation of small-world brain networks during a go/NoGo task. *Frontiers in Aging Neuroscience, 8*, 100.

Hornberger, M., Geng, J., & Hodges, J. R. (2011). Convergent grey and white matter evidence of orbitofrontal cortex changes related to disinhibition in behavioural variant frontotemporal dementia. *Brain, 134*(9), 2502–2512.

Hughes, M. M., Linck, J. A., Bowles, A. R., Koeth, J. T., & Bunting, M. F. (2014). Alternatives to switch-cost scoring in the task-switching paradigm: Their reliability and increased validity. *Behavior Research Methods, 46*(3), 702–721.

Inano, S., Takao, H., Hayashi, N., Abe, O., & Ohtomo, K. (2011). Effects of age and gender on white matter integrity. *American Journal of Neuroradiology, 32*(100), 2103–2109.

Jacobs, H. I., Leritz, E. C., Williams, V. J., Van Boxel, M. P., van der Elst, W., Jolles, J., et al. (2013). Association between white matter microstructure, executive functions, and processing speed in older adults: The impact of vascular health. *Human Brain Mapping, 34*(1), 77–95.

Jenkinson, M., & Smith, S. (2001). A global optimisation method for robust affine registration of brain images. *Medical Image Analysis, 5*(2), 143–156.

Jenkinson, M., Beckmann, C. F., Behrens, T. E., Woolrich, M. W., & Smith, S. M. (2012). Fsl. *Neuroimage, 62*(2), 782–790.

Jones, S. A., Butler, B. C., Kintzel, F., Johnson, A., Klein, R. M., & Eskes, G. A. (2016). Measuring the performance of attention networks with the Dalhousie computerized attention battery (DalCAB): Methodology and reliability in healthy adults. *Frontiers in Psychology, 7*, 823.

Kier, E. L., Staib, L. H., Davis, L. M., & Bronen, R. A. (2004). MR imaging of the temporal stem: Anatomic dissection tractography of the uncinate fasciculus, inferior occipitofrontal fasciculus, and Meyer's loop of the optic radiation. *American Journal of Neuroradiology, 25*(5), 677–691.

Kubicki, M., Niznikiewicz, M., Connor, E., Ungar, L., Nestor, P., Bouix, S., et al. (2009). Relationship between white matter integrity, attention, and memory in schizophrenia: A diffusion tensor imaging study. *Brain Imaging and Behavior, 3*(2), 191–201.

Lee, T., Mosing, M. A., Henry, J. D., Trollor, J. N., Lammel, A., Ames, D., Martin, N. G., Wright, M. J., & Sachdev, P. S. (2012). Genetic influences on five measures of processing speed and their covariation with general cognitive ability in the elderly: The older Australian twins study. *Behavior Genetics, 42*(1), 96–106.

Leemans, A., & Jones, D. K. (2009). The B-matrix must be rotated when correcting for subject motion in DTI data. *Magnetic Resonance in Medicine, 61*(6), 1336–1349.

Lu, P. H., Lee, G. J., Tishler, T. A., Meghpara, M., Thompson, P. M., & Bartzokis, G. (2013). Myelin breakdown mediates age-related slowing in cognitive processing speed in healthy older men. *Brain and Cognition, 81*(1), 131–138.

Madden, D. J., Bennett, I. J., & Song, A. W. (2009). Cerebral white matter integrity and cognitive aging: Contributions from diffusion tensor imaging. *Neuropsychology Review, 19*(4), 415–435.

Madden, D. J., Bennett, I. J., Burzynska, A., Potter, G. G., Chen, N. K., & Song, A. W. (2012). Diffusion tensor imaging of cerebral white matter integrity in cognitive aging. *Biochimica et Biophysica Acta, 1822*(3), 386–400.

Madden, D. J., Parks, E. L., Tallman, C. W., Boylan, M. A., Hoagey, D. A., Cocjin, S. B., Packard, L. E., Johnson, M. A., Chou, Y. H., Potter, G. G., Chen, N. K., Siciliano, R. E., Monge, Z. A., Honig, J. A., & Diaz, M. T. (2017). Sources of disconnection in neurocognitive aging: Cerebral white-matter integrity, resting-state functional connectivity, and white-matter hyperintensity volume. *Neurobiology of Aging, 54*, 199–213.

Marner, L., Nyengaard, J. R., Tang, Y., & Pakkenberg, B. (2003). Marked loss of myelinated nerve fibers in the human brain with age. *Journal of Comparative Neurology, 462*(2), 144–152.

Menon, V., Adleman, N. E., White, C. D., Glover, G. H., & Reiss, A. L. (2001). Error-related brain activation during a go/NoGo response inhibition task. *Human Brain Mapping, 12*(3), 131–143.

Metzler-Baddeley, C., Jones, D. K., Steventon, J., Westacott, L., Aggleton, J. P., & O'Sullivan, M. J. (2012). Cingulum microstructure predicts cognitive control in older age and mild cognitive impairment. *Journal of Neuroscience, 32*(49), 17612–17619.

Mori, S., & van Zijl, P. C. (2002). Fiber tracking: Principles and strategies - a technical review. *NMR Biomedicine, 15*(7–8), 468–480.

Murphy, C. F., Gunning-Dixon, F. M., Hoptman, M. J., Lim, K. O., Ardekani, B., Shields, J. K., Hrabe, J., Kanellopoulos, D., Shanmugham, B. R., & Alexopoulos, G. S. (2007). White-matter integrity predicts stroop performance in patients with geriatric depression. *Biological Psychiatry 61*(8):1007–1010.

O'Sullivan, M. R. C. P., Jones, D. K., Summers, P. E., Morris, R. G., Williams, S. C. R., & Markus, H. S. (2001). Evidence for cortical "disconnection" as a mechanism of age-related cognitive decline. *Neurology, 57*(4), 632–638.

Pan, S., & Chan, J. R. (2017). Regulation and dysregulation of axon infrastructure by myelinating glia. *The Journal of Cell Biology, 216*(12), 3903–3916.

Paul, R. H., Lawrence, J., Williams, L. M., Richard, C. C., Cooper, N., & Gordon, E. (2005). Preliminary validity of "integneuro": A new computerized battery of neurocognitive tests. *International Journal of Neurosciencei, 115*(11), 1549–1567.

Paul, R., Lane, E. M., Tate, D. F., Heaps, J., Romo, D. M., Akbudak, E., Niehoff, J., & Conturo, T. E. (2011). Neuroimaging signatures and cognitive correlates of the Montreal cognitive assessment screen in a nonclinical elderly sample. *Archives of Clinical Neuropsychology, 26*(5), 454–460.

Pavlov, I. Y., Wilson, A. R., & Delgado, J. C. (2010). Resampling approach for determination of the method for reference interval calculation in clinical laboratory practice. *Clinical and Vaccine Immunology, 17*(8), 1217–1222.

Phillips, O. R., Clark, K. A., Luders, E., Azhir, R., Joshi, S. H., Woods, R. P., Mazziotta, J. C., Toga, A. W., & Narr, K. L. (2013). Superficial white matter: Effects of age, sex, and hemisphere. *Brain Connectivity, 3*(2), 146–159.

Rizk, M. M., Rubin-Falcone, H., Keilp, J., Miller, J. M., Sublette, M. E., Burke, A., Oquendo, M. A., Kamal, A. M., Abdelhameed, M. A., & Mann, J. J. (2017). White matter correlates of impaired attention control in major depressive disorder and healthy volunteers. *Journal of Affective Disorders, 222*, 103–111.

Rubia, K., Russell, T., Overmeyer, S., Brammer, M. J., Bullmore, E. T., Sharma, T., Simmons, A., Williams, S. C. R., Giampietro, V., Andrew, C. M., & Taylor, E. (2001). Mapping motor inhibition: Conjunctive brain activations across different versions of go/no-go and stop tasks. *Neuroimage, 13*(2), 250–261.

Salat, D. H., Tuch, D. S., Greve, D. N., Van Der Kouwe, A. J. W., Hevelone, N. D., Zaleta, A. K., et al. (2005). Age-related alterations in white matter microstructure measured by diffusion tensor imaging. *Neurobiology of Aging, 26*(8), 1215–1227.

Salminen, L. E., Schofield, P. R., Lane, E. M., Heaps, J. M., Pierce, K. D., Cabeen, R., Laidlaw, D. H., Akbudak, E., Conturo, T. E., Correia, S., & Paul, R. H. (2013). Neuronal fiber bundle lengths in healthy adult carriers of the ApoE4 allele: A quantitative tractography DTI study. *Brain Imaging and Behavior, 7*(3), 274–281.

Salminen, L. E., Schofield, P. R., Pierce, K. D., Zhao, Y., Luo, X., Wang, Y., Laidlaw, D. H., Cabeen, R. P., Conturo, T. E., Tate, D. F., Akbudak, E., Lane, E. M., Heaps, J. M., Bolzenius, J. D., Baker, L. M., Cagle, L. M., & Paul, R. H. (2016). Neuromarkers of the common angiotensinogen polymorphism in healthy older adults: A comprehensive assessment of white matter integrity and cognition. *Behavioural Brain Resesarch, 296*, 85–93.

Salo, R., Nordahl, T. E., Buonocore, M. H., Natsuaki, Y., Waters, C., Moore, C. D., Galloway, G. P., & Leamon, M. H. (2009). Cognitive control and white matter callosal microstructure in methamphetamine dependent subjects: A DTI study. *Biological Psychiatry, 65*(2), 122–128.

Sasson, E., Doniger, G. M., Pasternak, O., Tarrasch, R., & Assaf, Y. (2013). White matter correlates of cognitive domains in normal aging with diffusion tensor imaging. *Frontiers in Neuroscience, 7*, 32.

Schmahmann, J. D., & Pandya, D. N. (2006). *Fiber pathways of the brain*. New York: Oxford University Press.

Sexton, C. E., Walhovd, K. B., Storsve, A. B., Tamnes, C. K., Westlye, L. T., Johansen-Berg, H., & Fjell, A. M. (2014). Accelerated changes in white matter microstructure during aging: A longitudinal diffusion tensor imaging study. *Journal of Neuroscience, 34*(46), 15425–15436.

Smith, S. M. (2002). Fast robust automated brain extraction. *Human Brain Mapping, 17*(3), 143–155.

Steele, V. R., Aharoni, E., Munro, G. E., Calhoun, V. D., Nyalakanti, P., Stevens, M. C., Pearlson, G., & Kiehl, K. A. (2013). A large scale (N = 102) functional neuroimaging study of response inhibition in a go/NoGo task. *Behavioural Brain Research, 256*, 529–536.

Sullivan, E. V., Rohlfing, T., & Pfefferbaum, A. (2010). Quantitative fiber tracking of lateral and interhemispheric white matter systems in normal aging: Relations to timed performance. *Neurobiology of Aging, 31*(3), 464–481.

Tang, Y., Nyengaard, J. R., Pakkenberg, B., & Gundersen, H. J. G. (1997). Age-induced white matter changes in the human brain: A stereological investigation. *Neurobiology of Aging, 18*(6), 609–615.

van Gaal, S., Ridderinkhof, K. R., Scholte, H. S., & Lamme, V. A. F. (2010). Unconscious activation of the prefrontal no-go network. *Journal of Neuroscience, 30*(11), 4143–4150.

Was, C. A., & Woltz, D. J. (2007). Reexamining the relationship between working memory and comprehension: The role of available long-term memory. *Journal of Memory and Language, 56*(1), 86–102.

Westlye, L. T., Walhovd, K. B., Dale, A. M., Bjørnerud, A., Due-Tønnessen, P., Engvig, A., et al. (2009). Life-span changes of the human brain white matter: Diffusion tensor imaging (DTI) and volumetry. *Cerebral Cortex, 20*(9), 2055–2068.

Woltz, D. J., & Was, C. A. (2006). Availability of related long-term memory during and after attention focus in working memory. *Memory & Cognition, 34*(3), 668–684.

Yang, J., Tian, X., Wei, D., Liu, H., Zhang, Q., Wang, K., Chen, Q., & Qiu, J. (2016). Macro and micro structures in the dorsal anterior cingulate cortex contribute to individual differences in self-monitoring. *Brain Imaging and Behavior, 10*(2), 477–485.

Yushkevich, P. A., Piven, J., Hazlett, H. C., Smith, R. G., Ho, S., Gee, J. C., & Gerig, G. (2006). User-guided 3D active contour segmentation of anatomical structures: Significantly improved efficiency and reliability. *Neuroimage, 31*(3), 1116–1128.

Zahr, N. M., Rohlfing, T., Pfefferbaum, A., & Sullivan, E. V. (2009). Problem solving, working memory, and motor correlates of association and commissural fiber bundles in normal aging: A quantitative fiber tracking study. *Neuroimage, 44*(3), 1050–1062.

Zhang, S., & Li, C. R. (2012). Functional networks for cognitive control in a stop signal task: Independent component analysis. *Human Brain Mapping, 33*(1), 89–104.

Zhang, S., Demiralp, C., & Laidlaw, D. H. (2003). Visualizing diffusion tensor MR images using streamtubes and streamsurfaces. *IEEE Transactions on Visualization and Computer Graphics, 9*(4), 454–462.

Zhang, H., Yushkevich, P. A., Alexander, D. C., & Gee, J. C. (2006). Deformable registration of diffusion tensor MR images with explicit orientation optimization. *Medical Image Analysis, 10*(5), 764–785.

Zhang, H., Yushkevich, P. A., Rueckert, D., & Gee, J. C. (2007, October). Unbiased white matter atlas construction using diffusion tensor images. In *International conference on medical image computing and computer-assisted intervention* (pp. 211–218). Berlin, Heidelberg: Springer.

Zhang, Y., Zhang, J., Oishi, K., Faria, A. V., Jiang, H., Li, X., et al. (2010). Atlas-guided tract reconstruction for automated and comprehensive examination of the white matter anatomy. *Neuroimage, 52*(4), 1289–1301.

Zhang, H., Schneider, T., Wheeler-Kingshott, C. A., & Alexander, D. C. (2012). NODDI: Practical in vivo neurite orientation dispersion and density imaging of the human brain. *Neuroimage, 61*(4), 1000–1016.